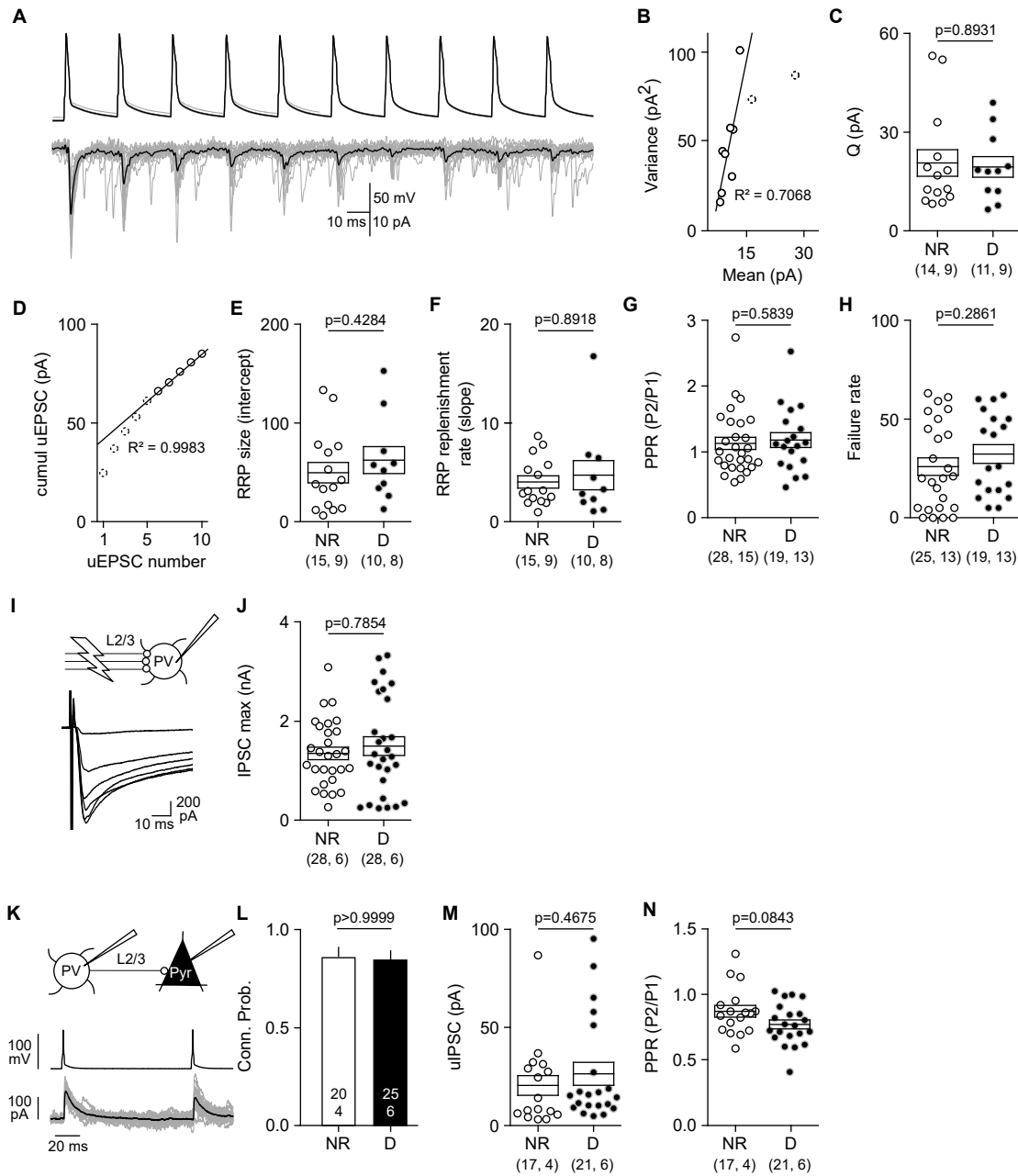
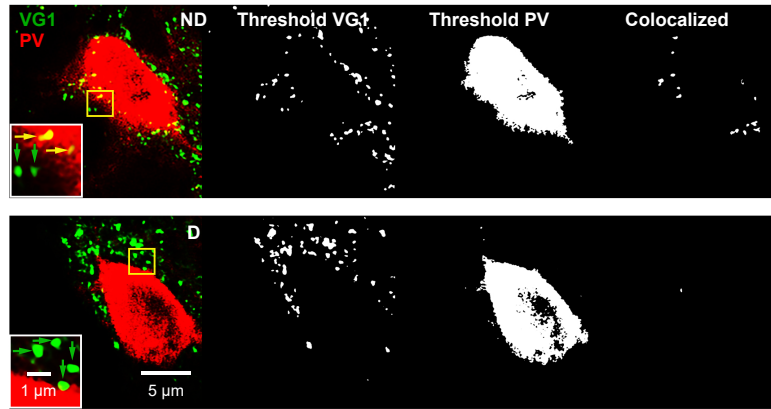


Supplementary Figure 1 (Figure 1 related)

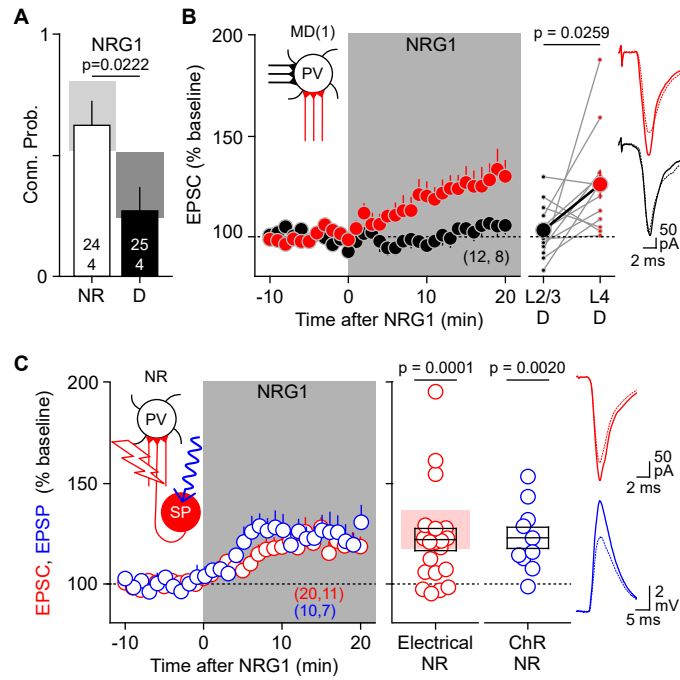


**Supplementary Fig. 1 | MD(1) only affects Pyr→PV probability of connection. (A-H)** MD(1) does not affect parameters of remaining Pyr→PV synapses. Synaptic parameters were estimated from the responses to 50 Hz trains (10 pulses). **A**, Superimposed traces show an example of 15 consecutive trials (gray) along with the averaged response (black). Scale bars: 50 mV, 10 pA, 20 ms. **B**, The example illustrates how the quantal size (Q), determined from the initial slope of a plot of mean uEPSC amplitude versus variance (see methods for more details). **C**, Q was not different in pairs from NR and D mice (MW-test  $U=74$ ,  $p=0.893$ ). **D**, The example illustrates how the linear relationship between the cumulative uEPSC amplitude vs stimulus number was used to estimate the readily releasable pool (RRP), size (intercept), and replenishment rate (slope), (Schneggenburger et al., 1999) see methods for details. **E,F**, MD(1) did not affect either the RRP size (**E**: MW-test  $U=60$ ,  $p=0.4284$ ) or the RRP replenishment rate (**F**: MW-test  $U=72$ ,  $p=0.892$ ). In addition, MD(1) did not affect the paired-pulse ratio (P2/P1) of the responses (**G**: MW-test  $U=240$ ,  $p=0.583$ ) or the uEPSC failure rate (**H**: MW-test  $U=192$ ,  $p=0.2861$ ). The number of cells or cell pairs and mice is indicated in parenthesis in **C-F**. **(I-N)** MD(1) does not affect the synaptic output of PV-Ins. **I-J**, MD(1) does not affect the inhibitory input onto PVs. **I**, Maximal IPSCs (IPSCmax) in L2/3 PVs were evoked by electrical stimulation series of increasing delivered ~100 $\mu$ m laterally. **J**, IPSCmax were not different in PV-Ins from NR and D mice (MW-test  $U=375$ ,  $p=0.7854$ ). **K-N**, MD(1) does not affect the PV-IN Pyr connectivity. **K** shows an example of uIPSCs (individuals: gray; average: black) evoked in a pyramidal cell (Pyr) by PV-IN firing. **L**, comparable connection probability in pairs from NR and D mice (F-test  $p>0.9999$ ). **M**, uIPSC amplitude in connected pairs from NR and D mice (MW-test  $U=153$ ,  $p=0.4675$ ). **N**, uIPSC paired pulse ratio (PPR: 100 ms interval) in connected pairs from NR and D mice (t-test  $F[31.5]=1.782$ ,  $p=0.0843$ ).



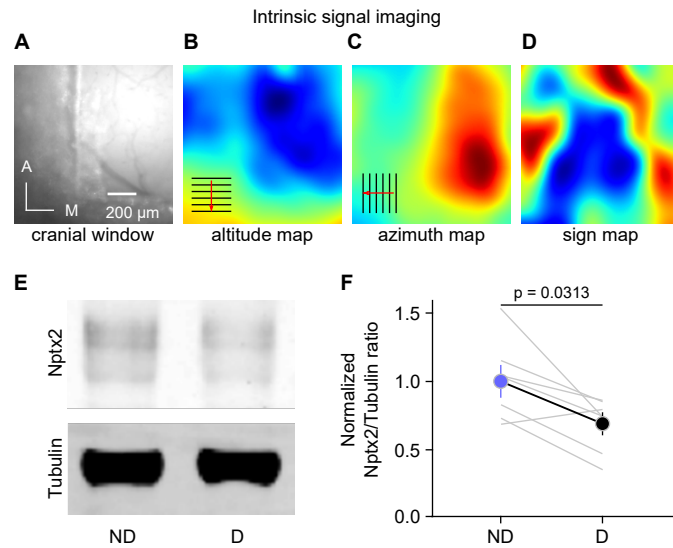
**Supplemental Fig.2 | Method for quantification of VGluT1 and PV co-localization.** Left, Example cases shown in Fig 2 (single z plane) showing PV in red, VG1 in green, 40X mag, area in yellow box magnified 2X in inset. Colocalized yellow puncta are identified with yellow arrows, non-colocalized puncta with green arrows. PV+ somata were identified by size exclusion ( $20\text{-}200\ \mu\text{m}^2$ ) and fluorescence intensity (auto threshold +25). Co-localization of VGluT1 puncta on PV somata were analyzed in single Z-section images taken at 40X, using Fiji. After the threshold function was applied to VGluT1 puncta (autothreshold +25), co-localized puncta were identified by size exclusion ( $0.1\ \mu\text{m}^2 < 2.0$  colocalized puncta that appear in more than 2 adjacent z sections were quantified).

Supplementary Figure 3 (Figure 3 related)

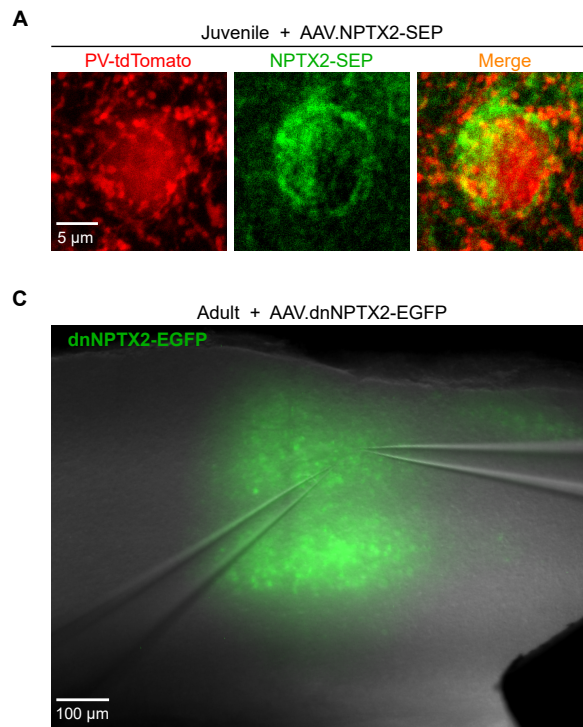


**Supplementary Fig. 3 | NRG1 does not affect inputs onto PVs from layer 2/3 Pyrs.** **A**, in mice between p21-25 systemically injected with NRG1 (1 $\mu$ g/mouse subcutaneous, 1X prior to eye suture and 1X 1h before sacrifice; MD(1) reduces the Pyr→PV connection probability. Gray bars indicate the 95% CI in non-injected mice (data from Fig 1). **B**, in slices from MD mice, superfusion of NRG1 (5 nM grey zone) selectively potentiated EPSCs evoked from layer 4 (red symbols: 126.0 $\pm$ 7.3% at 10-20 min. Wilcoxon test  $W=78$ ,  $p=0.0005$ ) without affecting EPSCs evoked from layer 3 (black symbols: 103.3 $\pm$ 3.9%, Wilcoxon test  $W=16$ ,  $p=0.5547$ ). Left: average time course; right: grey lines connect EPSCs evoked by layer 4 and layer 3 stimulation in the same cell; the black lines connect averages  $\pm$  s.e.m. **C**, NRG1 (5 nM grey zone) also potentiates EPSCs evoked by layer 4 stimulation in slices from normal-reared mice. Red symbols: electrically-evoked EPSCs; blue symbols: optogenetically-evoked EPSPs in mice expressing ChR2 in layer 4 (see methods). Left: average time course. Right: changes in individual cells; boxes: averages  $\pm$  s.e.m.; shaded red box: 95% C.I. for layer 4-evoked EPSCs in deprived slices (from 4b). Number of cells or cell pairs and mice is indicated in parenthesis in **A-C**.

Supplementary Figure 4 (Figure 3 related)

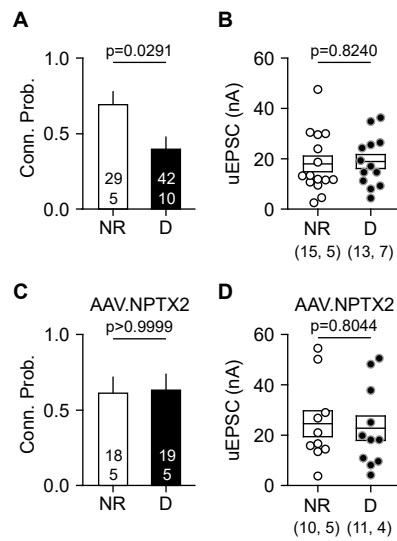


**Supplementary Fig. 4 | Supporting information on the quantification of changes in NPTX2.** (A-D) Localization of V1 with intrinsic signal imaging for the analysis of NPTX2-SEP. **A** The epifluorescence image of the cranial window. The black box area is where two-photon microscopy was performed. **B-D**, Altitude, azimuth, and sign map of the visual responses reveal the V1 region. The grids and arrows in **B,C** indicate the direction of visual stimulation. (E-F) Reduced NPTX2 protein content in V1 after MD(1). Western blot analysis of NPTX2 expression in the non-deprived (ND: open circle) and deprived (D: black circles) V1 of mice after 1 day of MD. NPTX2 levels were relativized to  $\beta$ -actin through densitometry analysis. **E**, example experiment. **F**; the grey lines connect data of individual mice. Circles connected by the thick line represent mean  $\pm$  SEM. Wilcoxon test  $W=-26$ ,  $p=0.0313$ .



**Supplementary Fig. 5 | Confirmation of viral transfection with AAV2-CaMKII-NPTX2-SEP and AAV2-CaMKII-dnNPTX2-EGFP. A**, AAV-CaMKII-NPTX2-SEP was injected into the visual cortex of PV-Cre;Ai14(tdTomato) newborn mice (p0-2). After 3-4 weeks, the effect of overexpressed NPTX-SEP on Pyr PV-IN connectivity and ODP were assessed. Expression of NPXT2-SEP in proximity of PV somas was confirmed by confocal microscopy. **B-C**, AAV-CaMKII-NPTX2-EGFP was injected into the same line of adult mice (p80-114). After 3-4 weeks, the effect of decreased expression of NPTX-SEP on Pyr PV-IN connectivity and ODP) was assessed. The expression of NPTX2-EGFP was detected on the slices (**B**) and through the cranial window (**C**).

Supplementary Figure 6 (Figure 1 and 3 related)



**Supplementary Fig. 6. | NPTX2 overexpression prevents MD-induced all or none loss of Pysr→PVinputs in the binocular region of V1 (V1b). A, B** In juvenile mice, (p21-p25) one day of MD reduces the Pyr→PV connection probability (**A**) without affecting the uEPSC amplitude of the connected pairs (**B**). t-test: 0.224, p=0.824 in juvenile. **C, D** In V1b juvenile mice, (p21-p25) transfected with AAV-CaMKII-NPTX2-SEP at birth one day of MD does not affect the connection probability (**C**) or the uEPSC amplitude of the connected pairs (**D**). Data is presented as averages ± s.e.m. The number of cells, pairs, and mice is indicated in parenthesis.